Available online at http://scik.org

Commun. Math. Biol. Neurosci. 2023, 2023:52

https://doi.org/10.28919/cmbn/7988

ISSN: 2052-2541

THE DYNAMICS OF A DELAYED ECOLOGICAL MODEL WITH PREDATOR REFUGE AND CANNIBALISM

REEM MUDAR HUSSIEN[1], RAID KAMEL NAJI[2,*]

[1]Biomedical Engineering Department, University of Technology, Baghdad, Iraq

[2]Department of Mathematics, College of Science, University of Baghdad, Iraq

Copyright © 2023 the author(s). This is an open access article distributed under the Creative Commons Attribution License, which permits unrestricted use, distribution, and reproduction in any medium, provided the original work is properly cited.

Abstract: This study has contributed to understanding a delayed prey-predator system involving cannibalism. The system is assumed to use the Holling type II functional response to describe the consuming process and incorporates the predator's refuge against the cannibalism process. The characteristics of the solution are discussed. All potential equilibrium points have been identified. All equilibrium points' local stability analyses for all time delay values are investigated. The system exhibits a Hopf bifurcation at the coexistence equilibrium, which is further demonstrated. The center manifold and normal form theorems for functional differential equations are then used to establish the direction of Hopf bifurcation and the stability of the periodic solution. To demonstrate the key findings, various numerical simulations are then run.

Keywords: prey-predator model; cannibalism; gestation delay; stability; Hopf-bifurcation.

2020 AMS Subject Classification: 34C23, 34D20, 92D30.

1. INTRODUCTION

Because predators are the main cause of prey death, prey is strongly selected to evolve more effective methods of spotting, avoiding, or fending off predators. The population of predators declines exponentially in the absence of prey species, forcing predators to develop better tracking

*Corresponding author

E-mail address: rknaji@gmail.com

Received April 14, 2023

and killing techniques or to look for new food sources. Since the predator population derives its energy from its species and can thus exist without its lone prey, we develop the model by taking cannibalism into account. In some mantises, fish, carnivore mammals, and spiders, cannibalism, also known as intraspecific predation, refers to devouring offspring or siblings. This occurrence is sometimes referred to as the "lifeboat mechanism" since it prevents a predator community from going extinct. Depending on the cannibalism rate, cannibalism can positively or negatively impact population abundance. This has sparked the interest of many academics in their research and produced a number of notable research findings. Therefore, for certain cannibals, including cannibalism in a stage-structured paradigm makes more sense. [1-7].

There is a delay in the appearance of some species' behavior in the natural ecosystem. In biological systems, the influence of a population on its condition has frequently been described using time delays. Delay differential equations are frequently more practical than regular differential equations in physics, ecology, biology, and other applications because a time delay could make an equilibrium that was previously stable unstable and induce population fluctuations. In the current work, the notion that energy obtained by eating food does not occur instantly is included. The functional response of the Holling type frequently displays this as a time delay. In delayed predator-prey models, the time delay may have an impact on the stability or instability of the prey densities as a result of predation. [8-11]. Due to new ecological evidence and theoretical advancements, there has been a recent increase in interest in various aspects of modeling biological interactions. Holling [12] proposed a more accurate illustration, which has since become one of the most widely used in ecology. It takes into account the hunt for prey and the handling of prey, two different components of the relationship between prey and predators. Functional responses may be influenced by a variety of ecological parameters, including prey habitat structure, predator hunting skills, and prey escape mechanisms [13]. Actually, the Holling type-II functional response, which is based on the traditional Lotka-Volterra model, is a function that increases, concave, smooths out, and saturates at high prey numbers. Numerous writers have examined this kind of functional response in predator-prey models, both with and without time delays even with spatial dependency [11, 14-15] and the references therein.

The occurrence of cannibalism is affected by a number of factors, including temperature, population density, developmental stage, and prey (predator) refuge [16]. You could argue that cannibalized predators have the ability to seek refuge from cannibalistic predators. By lowering the likelihood of extinction as a result of excessive predation, the refuge is an anti-predator

behavior that can aid in extending a predator-cannibalism relationship. When a predator detects cannibalism, they prepare for an attack by altering their behavior, including body shape, size, color, and habitat. It becomes particularly intriguing to research the delayed interactions between predator and prey, including predator cannibalism and predator refuge [4, 7, 17]. The present article modifies an ecological model with logistic growth in the prey to incorporate cannibalism in the predator and refuge with a temporal delay. The remainder of this paper is structured as follows. The mathematical model is built in section 2. In section 3, the prerequisites for equilibrium points' existence are established. In section 4, it is examined if each possible equilibrium of the system is locally stable. Section 5 studies the occurrence of Hopf bifurcation around the positive point. The direction of the Hopf bifurcation and the stability of the bifurcated periodic solutions are established in Section 6. Finally, Present some numerical findings and explore their biological implications in Sections 7 and 8.

2. MODEL CONSTRUCTION

The following model, which depicts a Lotka-Volterra prey-predator with predator cannibalism, was put forth by Deng et al. [4].

$$\begin{aligned} \frac{du}{dt} &= ru\left(1-\frac{u}{K}\right) - a_1uv, \\ \frac{dv}{dt} &= a_2uv + b_1v - cv - \frac{b_2v^2}{\beta+v}, \end{aligned} \tag{1}$$

where prey and predator density are denoted by $u \geq 0$ and $v \geq 0$. The parameters r, K, a_1, a_2, b_1, c, b_2, and β are positive constants that, respectively, represent the intrinsic growth rate of the prey, the carrying capacity of the prey in the environment, the rate of predation, the rate at which prey biomass is converted into predator birth, the rate at which cannibalism is converted into predator birth, the rate at which predators die, the rate at which cannibalism occurs within predator individuals, and the cannibalism half-saturation constant. The final term and the second term in the second equation of the system represent the cannibalism phenomena (1)

A model explaining the prey-predator interaction that incorporates predator cannibalism and refuge was recently proposed by Rayungsari et al [7], and then the proposed model underwent a dynamic study. By employing the Holling type II functional response rather than a Lotka-Volterra type of functional response and assuming that there is predator refuge from cannibalization, the suggested Rayungsari's model (2) is an improvement on Deng's model. The saturation predation mechanism is essentially described by the Holling type II functional response.

$$\begin{aligned} \frac{du}{dt} &= ru\left(1-\frac{u}{K}\right)-\frac{a_1 u\, v}{\beta_1+u}, \\ \frac{dv}{dt} &= \frac{a_2 u\, v}{\beta_1+u}+b_1 v-cv-\frac{b_2(1-m)v^2}{\beta_2+(1-m)v}, \end{aligned} \tag{2}$$

where β_1, β_2, and m are positive constants that, respectively, represent the predation half-saturation constant, the cannibalism half-saturation constant, and the predator refuge constant. While the other parameters are described above.

In actuality, although hunted victims are transformed into predator growth, there is a delay in predator biomass production due to the gestation period. Therefore, model (2) is altered by assuming that a continuous temporal lag known as gestation delay $\tau \in \mathbb{R}_+$ governs the reproduction of predator populations. Consequently, the new system is expressed as follows:

$$\begin{aligned} \frac{du}{dt} &= ru\left(1-\frac{u}{K}\right)-\frac{a_1 uv}{\beta_1+u}, \\ \frac{dv}{dt} &= \frac{a_2 u(t-\tau)v(t-\tau)}{\beta_1+u(t-\tau)}+b_1 v-cv-\frac{b_2(1-m)v^2}{\beta_2+(1-m)v}, \end{aligned} \tag{3}$$

where the system's (3) initial conditions are

$$u(\vartheta)=\varphi_1(\vartheta)>0, v(\vartheta)=\varphi_2(\vartheta)>0; \vartheta\in[-\tau,0]; \tag{4}$$

where $\varphi_i: C([-\tau,0]\rightarrow \mathbb{R}_+^2)$, for $i=1,2$. Here, C represents the Banach space of all continuous functions φ with the norm $\|\varphi\|=\underset{-\tau\le\vartheta\le 0}{Sup}\{|\varphi_1(\vartheta)|,|\varphi_2(\vartheta)|\}$.

Now, since the variables in system (3) represent the population densities, hence prey-predator populations must be constrained due to the limited carrying capacity of the prey and predator resources. So, the solution of system (3) must be nonnegative and uniformly bounded as shown in the following theorem.

Theorem 1: All the solutions of the system (3) with initial conditions (4) are positive and uniformly bounded in the interior of $\mathbb{R}_+^2$.

Proof: Because the functions on the right-hand side of the system (3) are continuous and satisfy the local Lipschitz condition on the continuous functions space C. Hence the solution $\big(u(t),v(t)\big)$ of the system (3) exists and is unique with the positive initial conditions (4) on $[0,\alpha)$, where $0<\alpha<\infty$ [4].

Now, from the initial value problem given by equations (3) and (4), it is obtained that:

$$u(t)=u(0)\,exp\int_0^t\left[r\left(1-\frac{u(\varepsilon)}{K}\right)-\frac{a_1\, v(\varepsilon)}{\beta_1+u(\varepsilon)}\right]d\varepsilon\ ,$$

$$v(t) = v(0)\, exp \int_0^t \left[\frac{a_2\, u(\varepsilon-\tau)v(\varepsilon-\tau)}{\beta_1+u(\varepsilon-\tau)} + b_1 - c - \frac{b_2(1-m)v(\varepsilon)}{\beta_2+(1-m)v(\varepsilon)}\right] d\varepsilon$$

Therefore, all the solutions of system (3) are positive. Now, to prove the boundedness of the solutions of the system (3) for all $t \geq 0$, we consider

$$V(t,\tau) = c_1 u(t-\tau) + c_2 v(t),$$

where c_1, and c_2 are positive constants. Simple calculations lead to

$$V' < r c_1 u(t-\tau) - \frac{r c_1 u^2(t-\tau)}{K} + \frac{(c_2 a_2 - c_1 a_1)u(t-\tau)v(t-\tau)}{\beta_1+u(t-\tau)} + c_2(b_1-c)v.$$

Set $c_1 = a_2$ and $c_2 = a_1$, then

$$V' < r a_2 u(t-\tau) - \frac{r a_2 u^2(t-\tau)}{K} + a_1(b_1-c)v.$$

For any positive M, such that

$$V' + MV < r a_2 u(t-\tau) - \frac{r a_2 u^2(t-\tau)}{K} + a_1(b_1-c)v + M(a_2 u(t-\tau) + a_1 v(t))$$
$$= a_2(r+M)u(t-\tau) - \frac{r a_2 u^2(t-\tau)}{K} + a_1(b_1-c+M)v$$

Take $M < c - b_1$, it is obtained that

$$V' + MV < a_2(r+M)u(t-\tau) - \frac{r a_2 u^2(t-\tau)}{K} = f(u(t-\tau))$$

Since $f''\big(u(t-\tau)\big) = -\frac{2ra_2}{K} < 0$ then $f(u(t-\tau))$ has maximum value given by $\frac{a_2 K(r+M)^2}{4r}$. This implies $V(t,\tau)$ is bounded and so are $u(t)$ and $v(t)$. Hence the proof is done.

3. THE EXISTENCE OF EQUILIBRIUM POINTS

The non-negative equilibrium points of the system (3) are determined, and the following four equilibrium points are obtained:

The trivial equilibrium point $P_0 = (0,0)$ and predator-free point $P_1 = (u_1, 0)$, where $u_1 = K$, exist unconditionally in $\mathbb{R}^2_+$.

The prey- free point $P_2 = (0, v_1)$, where $v_1 = \frac{\beta_2(c-b_1)}{(1-m)(b_1-c-b_2)}$, exists biologically in $\mathbb{R}^2_+$ if the following condition holds.

$$c < b_1 < b_2 + c \tag{5}$$

In other words, even if the prey is extinct, the predator will continue to exist as long as the rate of cannibalism conversion is higher than the rate of the predator's death and lower than the total rates of cannibalism and conversion.

The coexistence equilibrium point $P_3 = (u^*, v^*)$, where

$$v^* = \frac{r}{a_1}\left(1 - \frac{u^*}{K}\right)(\beta_1 + u^*) \tag{6}$$

while u^* represents the positive root of the following third-order polynomial equation:

$$A_1 u^3 + A_2 u^2 + A_3 u + A_4 = 0, \tag{7}$$

where

$$A_1 = (1-m)r(c - a_2 - b_1 + b_2).$$
$$A_2 = (1-m)r[-k(c - a_2 - b_1 + b_2) + \beta_1(2c - a_2 - 2b_1 + 2b_2)].$$
$$A_3 = [-k(1-m)r\beta_1(2c - a_2 - 2b_1 + 2b_2) + (1-m)r\beta_1^2(c - b_1 + b_2) - ka_1\beta_2(c + a_2 + b_1)].$$
$$A_4 = -(1-m)rk\beta_1^2(c - b_1 + b_2) - ka_1\beta_1\beta_2(c - b_1).$$

Clearly, according to Descartes' rule of signs, equation (7) has a unique positive root and hence system (3) has a unique coexistence equilibrium point if and only if the following sufficient condition is met.

$$c + b_2 < a_2 + b_1, \tag{8}$$

with one set of the following sets of conditions.

$$\left.\begin{matrix} A_2 < 0,\ A_4 > 0 \\ A_3 > 0,\ A_4 > 0 \end{matrix}\right\}. \tag{9}$$

4. LOCAL STABILITY

To study the local stability behavior of the equilibrium points, a linearization technique around an arbitrary equilibrium point is applied, resulting in the Jacobian matrix, which is then computed at each equilibrium point.

Let $P = (\bar{u}, \bar{v})$ be an arbitrary equilibrium point of the system (3). Then by considering the transformation $u_1(t) = u(t) - \bar{u}, u_2(t) = v(t) - \bar{v}$ respectively, hence after removing the bar, system (3) can be written as the following linear system.

$$\begin{aligned} \frac{du_1}{dt} &= f_{10}^{(1)} u_1(t) + f_{01}^{(1)} u_2(t), \\ \frac{du_2}{dt} &= f_{010}^{(2)} u_1(t-\tau) + f_{100}^{(2)} u_2(t) + f_{001}^{(2)} u_2(t-\tau), \end{aligned} \tag{10}$$

Where

$$\begin{aligned} f_{10}^{(1)} &= r - \frac{2ru}{K} - \frac{\beta_1 a_1 v}{(\beta_1+u)^2}, f_{01}^{(1)} = -\frac{a_1 u}{\beta_1+u}, \\ f_{010}^{(2)} &= \frac{\beta_1 a_2 v}{(\beta_1+u)^2}, f_{100}^{(2)} = b_1 - c - \frac{b_2(1-m)v(2\beta_2+(1-m)v)}{(\beta_2+(1-m)v)^2}, \\ f_{001}^{(2)} &= \frac{a_2 u}{\beta_1+u}, \end{aligned} \tag{11}$$

With

$$f^{(1)}(u_1,u_2)=ru_1+r\bar{u}-\frac{ru_1^2+2ru_1\bar{u}+r\bar{u}^2}{K}-\frac{a_1(u_2+\bar{v})(u_1+\bar{u})}{\beta_1+u_1+\bar{u}}.$$

$$f^{(2)}(u_2,u_1(t-\tau),u_2(t-\tau))=\frac{a_2(u_2(t-\tau)+\bar{v})(u_1(t-\tau)+\bar{u})}{\beta_1+u_1(t-\tau)+\bar{u}}$$

$$+(b_1-c)(u_2+\bar{v})-\frac{b_2(1-m)(u_2+\bar{v})^2}{\beta_2+(1-m)(u_2+\bar{v})}.$$

Then the characteristic equation of the system (3) at $P=(\bar{u},\bar{v})$ can be determined by

$$\begin{vmatrix} f_{10}^{(1)}-\lambda & f_{01}^{(1)} \\ f_{010}^{(2)}e^{-\lambda\tau} & (f_{100}^{(2)}+f_{001}^{(2)}e^{-\lambda\tau})-\lambda \end{vmatrix}=0 \tag{12}$$

The local stability around the equilibrium points of the system (3) is determined by the eigenvalues of the characteristic equation (12) and the result is obtained in the following theorem.

Theorem 2: The trivial equilibrium point $P_0=(0,0)$ is an unstable point for all $\tau\geq 0$.

Proof: Substituting $P_0=(0,0)$ in the general characteristic equation (12) gives that

$$\begin{vmatrix} r-\lambda & 0 \\ 0 & (b_1-c)-\lambda \end{vmatrix}=0. \tag{13}$$

Therefore, the eigenvalues of the system (3) at P_0 are $\lambda_{01}=r>0$, and $\lambda_{02}=b_1-c$.

Then, if $b_1>c$ then P_0 is a source, and if $b_1<c$ then P_0 is a saddle point. So, P_0 is always unstable for all $\tau\geq 0$.

Now before the next theorems are given, the following proposition that is given in [10] is presented.

Proposition 3: Suppose that $C_1>0$ and $C_2>0$, then the following is obtained

- If $C_1<C_2$, then all the roots of $\rho+C_1-C_2e^{-\rho\tau}=0$ have positive real parts for $\tau<\frac{1}{\sqrt{C_2^2-C_1^2}}\cos^{-1}\left(\frac{C_1}{C_2}\right)$.
- If $C_1>C_2$, then all the roots of $\rho+C_1-C_2e^{-\rho\tau}=0$ have negative real parts for any τ.

Theorem 4: The predator-free equilibrium point $P_1=(K,0)$ of the system (3) is asymptotically stable for $\tau\geq 0$ provided that the following condition is met

$$a_2<\frac{(c-b_1)(\beta_1+K)}{K}. \tag{14}$$

While it is unstable point for all $0\leq\tau<\tau_c=\frac{1}{\sqrt{\left(\frac{a_2K}{\beta_1+K}\right)^2-(c-b_1)^2}}\cos^{-1}\left(\frac{(c-b_1)(\beta_1+K)}{a_2K}\right)$ provided that condition (14) is reflected.

Proof: Substituting $P_1=(K,0)$ in the general characteristic equation (12) gives that

$$\begin{vmatrix} -r-\lambda & \frac{-a_1K}{\beta_1+K} \\ 0 & b_1-c+\frac{a_2K}{\beta_1+K}e^{-\lambda\tau}-\lambda \end{vmatrix}=0, \tag{15}$$

So the eigenvalues are $\lambda_{11}=-r<0$, while the other eigenvalues are given by the roots of the following transcendental equation:

$$\left(\frac{a_2K}{\beta_1+K}e^{-\lambda\tau}-(c-b_1)-\lambda\right)=0. \tag{16}$$

Clearly, for $\tau=0$, it is obtained $\lambda_{12}=\frac{a_2K}{\beta_1+K}+b_1-c$, which is a negative provided condition (14) holds, however, λ_{12} will be positive when the condition (14) is reflected. This makes P_1 a saddle point.

On the other hand, for $\tau>0$, due to proposition (3) all the roots of equation (16) have negative real parts roots or positive real parts roots for $\tau<\tau_c=\frac{1}{\sqrt{\left(\frac{a_2K}{\beta_1+K}\right)^2-(c-b_1)^2}}\cos^{-1}\left(\frac{(c-b_1)(\beta_1+K)}{a_2K}\right)$ when the condition (14) is satisfied or reflected respectively.

Consequently, the predator-free equilibrium point is locally asymptotically stable for all $\tau>0$ if the condition (14) is met, while it is an unstable point for $0<\tau<\tau_c$ when the condition (14) is reflected. This is complete the proof.

Theorem 5: The prey-free equilibrium point $P_2=(0,v_1)$ of the system (3) is locally asymptotically stable for all $\tau\geq 0$ if the following condition is met.

$$r<\frac{a_1v_1}{\beta_1}. \tag{17}$$

Proof: Substituting $P_2=(0,v_1)$ in the general characteristic equation (10) gives that

$$\begin{vmatrix} r-\frac{a_1v_1}{\beta_1}-\lambda & 0 \\ \frac{a_2v_1}{\beta_1}e^{-\lambda\tau} & b_1-c-\frac{b_2(1-m)v_1(2\beta_2+(1-m)v_1)}{(\beta_2+(1-m)v_1)^2}-\lambda \end{vmatrix}=0, \tag{18}$$

Therefore, the eigenvalues of the system (3) at P_2 are given by:

$$\lambda_{21}=r-\frac{a_1v_1}{\beta_1} \quad \text{and} \quad \lambda_{22}=b_1-c-\frac{b_2(1-m)v_1(2\beta_2+(1-m)v_1)}{(\beta_2+(1-m)v_1)^2}=\frac{(b_1-c)(b_1-c-b_2)}{b_2}.$$

Since λ_{22} is negative under the existing condition of P_2, which is given by equation (5). Then, P_2 is locally asymptotically stable if and only if condition (17) is met. While it is saddle point if that condition is reflected.

Theorem 6: The coexistence equilibrium point $P_3=(u^*,v^*)$ of the system (3) is locally asymptotically stable for all $0\leq\tau<\tau_0$ provided that the following condition is met.

$$K<\beta_1+2u^* \tag{19}$$

However, it is unstable point for $\tau_0 \leq \tau$ provided that

$$M^2 - S^2 < 0 \tag{20}$$

where all the new symbols are given in the proof.

Proof: The characteristic equation of the system (3) at P_3 is determined by equation (12), where $f_{10}^{(1)}$, $f_{01}^{(1)}$, $f_{100}^{(2)}$, $f_{010}^{(2)}$, and $f_{001}^{(2)}$ can be written as:

$$\begin{gathered} f_{10}^{(1)} = \frac{ru^*}{\beta_1+u^*}\left(1-\frac{\beta_1+2u^*}{K}\right), f_{01}^{(1)} = -\frac{a_1u^*}{\beta_1+u^*}, f_{010}^{(2)} = \frac{r\beta_1a_2}{a_1(\beta_1+u^*)}\left(1-\frac{u^*}{K}\right), \\ f_{100}^{(2)} = b_1 - c - \frac{b_2(1-m)v^*(2\beta_2+(1-m)v^*)}{(\beta_2+(1-m)v^*)^2}, f_{001}^{(2)} = \frac{a_2u^*}{\beta_1+u^*}. \end{gathered} \tag{21}$$

Now, according to the linear system (10) and their characteristic equation (12) at P_3, which can be rewritten in the following form:

$$\lambda^2 + N\lambda + M + e^{-\lambda\tau}(Q\lambda + S) = 0, \tag{22}$$

where

$$N = -(f_{10}^{(1)} + f_{100}^{(2)}),\ M = f_{10}^{(1)}f_{100}^{(2)},\ Q = -f_{001}^{(2)},\ S = f_{10}^{(1)}f_{001}^{(2)} - f_{01}^{(1)}f_{010}^{(2)}.$$

For $\tau = 0$, then the characteristic equation (22) becomes

$$\lambda^2 + (N+Q)\lambda + M + S = 0, \tag{23}$$

By substituting the value of $v^* = \frac{r}{a_1}\left(1-\frac{u^*}{K}\right)(\beta_1+u^*)$ in the forms $f_{100}^{(2)}$, and $f_{001}^{(2)}$ and simplifying the resulting terms, it is obtained that:

$$f_{001}^{(2)} + f_{100}^{(2)} = -\frac{a_1b_2\beta_2r(1-m)\left(1-\frac{u^*}{K}\right)(\beta_1+u^*)}{\left(a_1\beta_2+r(1-m)\left(1-\frac{u^*}{K}\right)(\beta_1+u^*)\right)^2} < 0. \tag{24}$$

Moreover, direct computation gives the following two expressions:

$$N + Q = -\left[f_{10}^{(1)} + (f_{001}^{(2)} + f_{100}^{(2)})\right],$$

$$M + S = f_{10}^{(1)}\left(f_{100}^{(2)} + f_{001}^{(2)}\right) - f_{01}^{(1)}f_{010}^{(2)},$$

which are positive under the condition (19), and the expression (24).

Hence, the coexistence equilibrium point is locally asymptotically stable for $\tau = 0$. That is, all the roots of equation (23) have negative real parts.

Now, when $0 < \tau$, by Butler's lemma [18], P_3 remains stable for $\tau < \tau_0$ where τ_0 is a specific value. Moreover, due to corollary 2.4 in Ruan and Wei [19], a characteristic root of equation (22) must intersect the imaginary axis if instability occurs for a specific value of the delay τ_0.

Consequently, it is assumed that equation (22) has a root that is entirely imaginary, $\lambda = i\theta$, with $\theta > 0$ to be exist. Then, by substituting it in equation (22), and then separating the real and imaginary components, it is obtained that:

$$Q\theta \sin\theta\tau + S\cos\theta\tau = \theta^2 - M, \quad (25)$$

$$Q\theta \cos\theta\tau - S\sin\theta\tau = -N\theta, \quad (26)$$

By squaring and adding (25) and (26), it is arrived the following algebraic equation of θ:

$$\theta^4 + \mathrm{H}_1\theta^2 + \mathrm{H}_2 = 0, \quad (27)$$

where $\mathrm{H}_1 = N^2 - Q^2 - 2M$, and $\mathrm{H}_2 = M^2 - S^2$.

Substituting $\theta^2 = X$ in (27) gives the following second-order equation:

$$f(X) = X^2 + \mathrm{H}_1 X + \mathrm{H}_2 = 0. \quad (28)$$

Clearly, by applying Descartes's rule of signs, we can say that equation (28), and hence (27) has at least one positive root $\theta_0 = \sqrt{X}$ if the condition (20) holds. Thus, for $\tau_0 \leq \tau$, the characteristic equation (22) has roots with a positive real part and hence P_3 becomes unstable.

In the following, the value of τ_0 at which the stability P_3 changed is determined. From equations (25) and (26), the following is reached.

$$\sin\theta\tau = \frac{\theta^2 - S\cos\theta\tau - M}{Q\theta},$$

$$\cos\theta\tau = \frac{S(\theta^2 - M) - QN\theta^2}{\mathrm{Q}^2\theta^2 + S^2}.$$

Then, τ_k corresponding to θ_0 can be obtained as

$$\tau_k = \frac{1}{\theta_0}\left(\cos^{-1}\frac{S(\theta^2 - M) - QN\theta^2}{\mathrm{Q}^2\theta^2 + S^2} + 2k\pi\right), k = 0,1,2,\ldots \quad (29)$$

Define

$$\tau_0 = \min\tau_k\,,\ k \geq 0, \quad (30)$$

This completes the proof of the theorem.

5. HOPF BIFURCATION ANALYSIS

In this section, the possibility of occurrence of Hopf bifurcation around the coexistence equilibrium point is discissed. From the above, it is proved that the characteristic equation (22) of the system (3) has a pair of complex conjugate roots, given by $\lambda = \gamma(\tau) \pm i\theta(\tau)$, which are pure imaginary at $\tau = \tau_0$ that is $\gamma(\tau_0) = 0$. Therefore, system (3) undergoes a Hopf bifurcation around the coexistence equilibrium point at $\tau = \tau_0$ if we can prove the transversality criterion

[20] that is given by $\left[\frac{d(Re\,\lambda(\tau))}{d\tau}\right]_{\tau=\tau_0} \neq 0$.

Theorem 7. System (3) undergoes a Hopf bifurcation around the coexistence equilibrium point at $\tau = \tau_0$ provided that the following condition is met.

$$\psi_1\Gamma_1 - \psi_2\Gamma_2 \neq 0, \tag{31}$$

where all the new symbols are given in the proof.

Proof. From the theorem (6), it is obtained that $P_3 = (u^*, v^*)$ of the system (3) is locally asymptotically stable for all $0 \leq \tau < \tau_0$, while it is unstable for $\tau_0 \leq \tau$ under certain given conditions with τ_0 is given by equation (30) that satisfy $Re\,\lambda(\tau_0) = 0$. Therefore in the neighborhood of τ_0 the complex eigenvalues can be represented as $\lambda = \gamma(\tau) \pm i\theta(\tau)$ with $\gamma(\tau_0) = 0$.

By substituting λ it in equation (22), and then separating the real and imaginary components, it is obtained that:

$$\gamma^2 - \theta^2 + N\gamma + (Q\gamma\cos\theta\tau + Q\theta\sin\theta\tau + S\cos\theta\,\tau)e^{-\gamma\tau} + M = 0,$$
$$2\gamma\theta + N\theta - (Q\gamma\sin\theta\tau - Q\theta\cos\theta\tau + S\sin\theta\,\tau)e^{-\gamma\tau} = 0,$$

Differentiating the above two equations with reference to τ and then substituting $\gamma = 0$, yields:

$$\begin{aligned}\Gamma_1(\tau)\frac{d\gamma}{d\tau} + \Gamma_2(\tau)\frac{d\theta}{d\tau} &= \psi_1(\tau),\\ -\Gamma_2(\tau)\frac{d\gamma}{d\tau} + \Gamma_1(\tau)\frac{d\theta}{d\tau} &= \psi_2(\tau),\end{aligned} \tag{32}$$

where

$$\Gamma_1 = Q\cos\theta\tau - Q\theta\tau\sin\theta\tau - S\tau\cos\theta\tau + N.$$
$$\Gamma_2 = Q\sin\theta\tau + Q\theta\tau\cos\theta\tau - S\tau\sin\theta\tau - 2\theta.$$
$$\psi_1 = Q\theta^2\cos\theta\tau - S\theta\sin\theta\tau.$$
$$\psi_2 = -Q\theta^2\sin\theta\tau - S\theta\cos\theta\tau.$$

Solving the linear algebraic system (32) for $\frac{d\gamma}{d\tau}$, gives that:

$$\left[\frac{d\gamma}{d\tau}\right]_{\tau=\tau_0} = \frac{\psi_1\Gamma_1 - \psi_2\Gamma_2}{\Gamma_1^2 + \Gamma_2^2}.$$

Clearly, $\left[\frac{d\gamma}{d\tau}\right]_{\tau=\tau_0} = \left[\frac{d(Re\lambda(\tau))}{d\tau}\right]_{\tau=\tau_0} \neq 0$ under the condition (31) that complete the proof.

6. DIRECTION AND STABILITY OF HOPF BIFURCATION

The explicit formulas that determine the direction, stability, and period of periodic trajectories bifurcating from equilibrium P_3 at critical values of delay τ_0 are derived as given in the following theorem and are based on the center manifold and normal form theory introduced by Hassard et al. [20].

Theorem 8. Under the following established fixed quantities, the stability and direction of the bifurcating periodic solution can be calculated.

$$\left.\begin{aligned} C_1(0) &= \frac{i}{2\theta\tau_0}\left(g_{11}g_{20} - 2\,|g_{11}|^2 + \frac{|g_{02}|^2}{3}\right) + \frac{g_{21}}{2} \\ \mu_2 &= -\frac{Re\{C_1(0)\}}{Re\left\{\frac{d\lambda(\tau^*)}{d\tau}\right\}} \\ \beta_2 &= 2\,Re\{C_1(0)\} \\ T_2 &= -\frac{Im\,\{C_1(0)\} + N_2\,Im\left\{\frac{d\lambda(\tau_0)}{d\tau}\right\}}{\theta\tau_0} \end{aligned}\right\} \tag{33}$$

Then, for system (3) around P_3 at critical point $\tau = \tau_0$, the physical characteristics of the Hopf bifurcation are listed below:

1. If $\mu_2 > 0$ $(\mu_2 < 0)$, then direction of the Hopf bifurcation is supercritical (sub-critical) and the bifurcating periodic trajectories exist for $\tau > \tau_0$ $(\tau < \tau_0)$.
2. If $\beta_2 > 0$ $(\beta_2 < 0)$, then the bifurcating periodic trajectories are stable (unstable).
3. If $T_2 > 0$ $(T_2 < 0)$, then the period of the bifurcating periodic trajectories increases (decreases).

Proof. System (3) produces the following functional differential equation in $C = C([-1,0], \mathbb{R}^2)$ by transforming the time delay using the linear transformations $u_1(t) = u(t) - u^*$, $u_2(t) = v(t) - v^*$, $\eta = \tau - \tau_0$, where $\eta \in \mathbb{R}$. The Hopf bifurcation point τ_0 that is defined in equation (30) is obviously reached at the value $\eta = 0$, and the periodic trajectories of system (3) are equivalent to those of the subsequent resultant system.

$$\frac{d\mathbf{u}(t)}{dt} = L_\eta(\mathbf{u}_t) + F(\eta\,, \mathbf{u}_t), \tag{34}$$

where $\mathbf{u}(t) = \mathbf{u}_t = \big(u_1(t), u_2(t)\big)^T \in \mathbb{R}^2$, and $L_\eta : C \longrightarrow \mathbb{R}^2$, and $F : \mathbb{R} \times C \longrightarrow \mathbb{R}^2$, with

$$L_\eta(\varphi) = (\tau_0 + \eta)\left[\begin{pmatrix} f_{10}^{(1)} & f_{01}^{(1)} \\ 0 & f_{100}^{(2)} \end{pmatrix}\begin{pmatrix} \varphi_1(0) \\ \varphi_2(0) \end{pmatrix} + \begin{pmatrix} 0 & 0 \\ f_{010}^{(2)} & f_{001}^{(2)} \end{pmatrix}\begin{pmatrix} \varphi_1(-1) \\ \varphi_2(-1) \end{pmatrix}\right], \tag{35}$$

with $f_{10}^{(1)}$, $f_{01}^{(1)}$, $f_{100}^{(2)}$, $f_{010}^{(2)}$, and $f_{001}^{(2)}$ are given in equation (11). While, the nonlinear term is given by

$$F(\eta, \varphi) = (\tau_0 + \eta)\begin{bmatrix} \sum_{i+j\geq 2} \frac{1}{i!j!}\, f_{ij}^{(1)}\, \varphi_1^i(0)\, \varphi_2^j(0) \\ \sum_{i+j+k\geq 2} \frac{1}{i!j!k!}\, f_{ijk}^{(2)}\, \varphi_2^i(0)\, \varphi_1^j(-1)\, \varphi_2^k(-1) \end{bmatrix}, \tag{36}$$

with $\boldsymbol{\varphi}(x) = \big(\varphi_1(x), \varphi_2(x)\big)^T \in C$, $x \in [-1, 0]$, while $f^{(1)}(\varphi_1, \varphi_2,)$, $f^{(2)}(\varphi_2, h_1, h_2)$,

$f_{ij}^{(1)}\varphi_1^i(0)\,\varphi_2^j(0)$, and $f_{ijk}^{(2)}\varphi_2^i(0)\,\varphi_1^j(-1)\varphi_2^k(-1)$ are given as follows, where $h_1=\varphi_1(-1)$, and $h_2=\varphi_2(-1)$.

$$f^{(1)}(\varphi_1,\varphi_2)=r\varphi_1+ru^*-\frac{r\varphi_1^2+2r\varphi_1u^*+ru^{*2}}{K}-\frac{a_1(\varphi_2+v^*)(\varphi_1+u^*)}{\beta_1+\varphi_1+u^*}$$

$$f^{(2)}(\varphi_2,h_1,h_2)=\frac{a_2(h_2+v^*)(h_1+u^*)}{\beta_1+h_1+u^*}+(b_1-c)(\varphi_2+v^*)-\frac{b_2(1-m)(\varphi_2+v^*)^2}{\beta_2+(1-m)(\varphi_2+v^*)},$$

$$f_{ij}^{(1)}=\left.\frac{\partial^{i+j}f^{(1)}}{\partial\varphi_1^i\,\varphi_2^j}\right|_{(\varphi_1,\varphi_2)=(0,0)},$$

$$f_{ijk}^{(2)}=\left.\frac{\partial^{i+j}f^{(2)}}{\partial\varphi_2^i\,h_1^j\,h_2^j}\right|_{(\varphi_2,h_1,h_2)=(0,-1,-1)}.$$

Additionally, direct computation yields the higher derivatives listed below.

$$\left.\begin{gathered}f_{11}^{(1)}=-\frac{a_1\beta_1}{(\beta_1+u^*)^2},f_{20}^{(1)}=-\frac{2r}{K}+\frac{a_1v^*(1+2u^*)}{(\beta_1+u^*)^3},f_{02}^{(1)}=0,\\ f_{200}^{(2)}=\frac{(\beta_2+(1-m)v^*)[6b_2(1-m)^2v^*]-2b_2(1-m)^3v^{*2}}{(\beta_2+(1-m)v^*)^3},\ f_{020}^{(2)}=-\frac{2\beta_1a_2v^*}{(\beta_1+u^*)^3},f_{002}^{(1)}=0,\\ f_{110}^{(2)}=0,f_{101}^{(2)}=0,f_{011}^{(2)}=\frac{a_2u^*}{(\beta_1+u^*)^2}.\end{gathered}\right\}\tag{37}$$

According to the Riesz representation theorem [20], a 2×2 matrix denoted by $\Pi(x,\eta)$ exists with inputs that are bounded variation functions in such a way that

$$L_\eta\boldsymbol{\varphi}=\int_{-1}^{0}[d\Pi(x,\eta)]\boldsymbol{\varphi}(x),\text{ for }\boldsymbol{\varphi}\in C.\tag{38}$$

In fact, it can be choose

$$\Pi(x,\eta)=(\tau_0+\eta)\left[\begin{pmatrix}f_{10}^{(1)}&f_{01}^{(1)}\\0&f_{100}^{(2)}\end{pmatrix}\delta(x)-\begin{pmatrix}0&0\\f_{010}^{(2)}&f_{001}^{(2)}\end{pmatrix}\delta(x+1)\right],\tag{39}$$

where $\delta(x)$ denotes the Dirac delta function and is defined as

$$\delta(x)=\begin{cases}1, & x=0\\0, & x\neq0\end{cases}.$$

For $\boldsymbol{\varphi}\in C^1([-1,0],\mathbb{R}^2)$, define that

$$A(\eta)\boldsymbol{\varphi}(x)=\begin{cases}\frac{d\varphi(x)}{dx}; & x\in[-1,0)\\ \int_{-1}^{0}[d\Pi(x,\eta)]\,\varphi(x); & x=0\end{cases},\tag{40}$$

and

$$R(\eta)\boldsymbol{\varphi}(x)=\begin{cases}0; & x\in[-1,0)\\ f(\eta,\boldsymbol{\varphi}); & x=0\end{cases}.\tag{41}$$

Thus, system (34) is corresponding to

$$\frac{d\mathbf{u}(t)}{dt} = A(\eta)\,\mathbf{u}_t + R(\eta)\,\mathbf{u}_t, \tag{42}$$

where $\mathbf{u}_t(x) = \mathbf{u}(t+x)$ for $x \in [-1,0]$. Furthermore, for $\boldsymbol{\psi} \in C^1([0,1],(\mathbb{R}^2)^*)$, define

$$A^*\boldsymbol{\psi}(s) = \begin{cases} -\frac{d\boldsymbol{\psi}(s)}{ds}; & s \in (0,1] \\ \int_{-1}^{0} [d\Pi^T(t,0)]\,\boldsymbol{\psi}(-t); & s = 0 \end{cases}, \tag{43}$$

where Π^T represents the transpose matrix Π. For $\boldsymbol{\varphi} \in C^1([-1,0],\mathbb{R}^2)$ and $\boldsymbol{\psi} \in C^1([0,1],(\mathbb{R}^2)^*)$, the next bilinear inner product is defined below to normalize the eigenvectors of operator A and adjoint operator A^*.

$$\langle \boldsymbol{\psi}(s), \boldsymbol{\varphi}(x)\rangle = \bar{\boldsymbol{\psi}}(0)\,\boldsymbol{\varphi}(0) - \int_{-1}^{0}\int_{\epsilon=0}^{x} \bar{\boldsymbol{\psi}}(\epsilon - x)\,d\Pi(x)\,\boldsymbol{\varphi}(\epsilon)\,d\epsilon, \tag{44}$$

where $\Pi(x) = \Pi(x,0)$. Obviously, $A = A(0)$ and $A^* = A^*(0)$ are adjoint operators, then it is obtained that $\langle \boldsymbol{\psi}, A\boldsymbol{\varphi}\rangle = \langle A^*\boldsymbol{\psi}, \boldsymbol{\varphi}\rangle$.

Now, since the system (34) undergoes a Hopf bifurcation near equilibrium point P_3. Then system (34) has two pure imaginary eigenvalues $\mp i\theta\tau_0$ of A, which are also eigenvalues of A^*.

Now, by a simple calculation, the eigenvectors of $A(0)$ and A^* associated with the eigenvalues $\mp i\theta\tau_0$ are computed, respectively, as follows:

$$\left.\begin{array}{l} q(x) = (1,q_1)^T e^{i\theta\tau_0 x} \\ q^*(s) = D(1,q_1^*)^T e^{-i\theta\tau_0 s} \end{array}\right\}, \tag{45}$$

where

$$\left.\begin{array}{l} q_1 = -\frac{f_{010}^{(2)}\, e^{-i\tau_0\theta}}{f_{100}^{(2)} + f_{001}^{(2)} e^{-i\tau_0\theta}} \\ q_1^* = -\frac{f_{01}^{(1)}}{f_{100}^{(2)} + f_{001}^{(2)} e^{-i\tau_0\theta}} \end{array}\right\}. \tag{46}$$

Moreover, determine the parameter value of D, such that:

$$\langle q^*(s), q(x)\rangle = 1;\ \langle q^*(s), \bar{q}(x)\rangle = 0. \tag{47}$$

According to equation (44), it is observed that:

$$\langle q^*(s), q(x)\rangle = \bar{D}\left(1,\overline{q_1^*}\right)(1,q_1)^T - \int_{-1}^{0}\int_{\epsilon=0}^{x} \bar{D}\left(1,\overline{q_1^*}\right) e^{-i\theta\tau_0(\epsilon - x)}\, d\Pi(x)(1,q_1)^T e^{i\theta\tau_0\epsilon}\, d\epsilon$$

$$= \bar{D}\left(1 + q_1\,\overline{q_1^*} + \tau_0\,\overline{q_1^*}\left(f_{010}^{(2)} + q_1\, f_{001}^{(2)}\right) e^{\,i\theta\tau_0}\right)$$

Therefore, due to (47), it is obtained that

$$\left.\begin{aligned}\overline{D} &= \left(1 + q_1\,\overline{q_1^*} + \tau_0\,\overline{q_1^*}\left(f_{010}^{(2)} + q_1\,f_{001}^{(2)}\right)e^{\,i\theta\tau_0}\right)^{-1}\\ D &= \left(1 + \overline{q_1}q_1^* + \tau_0 q_1^*\left(f_{010}^{(2)} + \overline{q_1}\,f_{001}^{(2)}\right)e^{\,i\theta\tau_0}\right)^{-1}\end{aligned}\right\} \tag{48}$$

Moreover, from the adjoining property $\langle \boldsymbol{\psi}, A\boldsymbol{\varphi}\rangle = \langle A^*\boldsymbol{\psi}, \boldsymbol{\varphi}\rangle$, it follows that $\langle q^*(s), \bar{q}(x)\rangle = 0$.

The characteristics of the bifurcating periodic trajectories of the system (34) can then be explored and evaluated using a method similar to that in [20]. In the following, the coefficients g_{ij} determine the stability and direction of the Hopf bifurcation are listed.

$$\left.\begin{aligned} g_{20} &= 2\,\tau_0\,\overline{D}\left(R_1 + \overline{q_1^*}\,R_5\right)\\ g_{11} &= \tau_0\;\overline{D}\left(R_2 + \overline{q_1^*}\,R_6\right)\\ g_{02} &= 2\tau_0\,\overline{D}\left(R_3 + \overline{q_1^*}\,R_7\right)\\ g_{21} &= 2\tau_0\,\overline{D}\left(R_4 + \overline{q_1^*}\,R_8\right)\end{aligned}\right\}, \tag{49}$$

where

$$R_1 = q_1\,f_{11}^{(1)} + f_{20}^{(1)},$$

$$R_2 = 2\,f_{20}^{(1)} + (q_1 + \overline{q_1})\;f_{11}^{(1)},$$

$$R_3 = \overline{q_1}\;f_{11}^{(1)} + f_{20}^{(1)},$$

$$R_4 = f_{11}^{(1)}\left(q_1 w_{11}^{(1)}(0) + \tfrac{1}{2}\,\bar{q}_1 w_{20}^{(1)}(0) + \tfrac{1}{2}\,w_{20}^{(2)}(0) + w_{11}^{(2)}(0)\right) + f_{20}^{(1)}\left(w_{20}^{(1)}(0) + 2w_{11}^{(1)}(0)\right),$$

$$R_5 = q_1 e^{-2i\theta\tau_0}\,f_{011}^{(2)} + q_1^2\,f_{200}^{(2)} + e^{-2i\theta\tau_0}\,f_{020}^{(2)},$$

$$R_6 = 2\,f_{020}^{(2)} + 2q_1\overline{q_1}\;f_{200}^{(2)} + (q_1 + \overline{q_1})\,f_{011}^{(2)},$$

$$R_7 = \overline{q_1}\,e^{2i\theta\tau_0} f_{011}^{(2)} + \overline{q_1^2}\,f_{200}^{(2)} + e^{2i\theta\tau_0} f_{020}^{(2)},$$

$$R_8 = K_1\,f_{011}^{(2)} + K_2\,f_{200}^{(2)} + K_3\,f_{020}^{(2)},$$

with,

$$K_1 = \tfrac{1}{2}\overline{q_1}\,W_{20}^{(1)}(-1)e^{i\theta\tau_0} + q_1\,W_{11}^{(1)}(-1)e^{-i\theta\tau_0} + W_{11}^{(2)}(-1)e^{-i\theta\tau_0} + \tfrac{1}{2}W_{20}^{(2)}(-1)e^{i\theta\tau_0},$$

$$K_2 = \overline{q_1}\,W_{20}^{(1)}(0) + 2q_1\,W_{11}^{(1)}(0),$$

$$K_3 = W_{20}^{(1)}(-1)e^{i\theta\tau_0} + 2\,W_{11}^{(1)}(-1)e^{-i\theta\tau_0},$$

Clearly, the values of g_{20}, g_{11}, and g_{02} can be determined from the above findings, while g_{21} needs to determine $W_{20}(x)$ and $W_{11}(x)$. So, performing certain arithmetic procedures and solving for $W_{20}(x)$ and $W_{11}(x)$ yields:

$$\left.\begin{aligned} W_{20}(x) &= \frac{ig_{20}}{\theta\tau_0}q(0)\,e^{\,i\theta\tau_0 x} + \frac{i\,\overline{g_{11}}}{3\theta\tau_0}\bar{q}(0)\,e^{-i\theta\tau_0 x} + U_1\,e^{\,2i\theta\tau_0 x} \\ W_{11}(v) &= -\frac{ig_{11}}{\theta\tau_0}q(0)\,e^{\,i\theta\tau_0 x} + \frac{i\,\overline{g_{02}}}{\theta\tau_0}\bar{q}(0)\,e^{-i\theta\tau_0 x} + U_2 \end{aligned}\right\}, \tag{50}$$

where $U_i = \left(U_i^{(1)}, U_i^{(2)}\right)^T \in \mathbb{R}^2$ for $i = 1,2$ are constant vectors, which can be determined from the following equations:

$$\begin{bmatrix} 2i\theta - f_{10}^{(1)} & -f_{01}^{(1)} \\ -f_{010}^{(2)}\,e^{\,2i\theta\tau_0} & 2i\theta - (f_{100}^{(2)} + f_{001}^{(2)}\,e^{\,2i\theta\tau_0}) \end{bmatrix} \begin{bmatrix} U_1^{(1)} \\ U_1^{(2)} \end{bmatrix} = 2\begin{bmatrix} R_1 \\ R_5 \end{bmatrix}. \tag{51}$$

$$\begin{bmatrix} -f_{10}^{(1)} & -f_{01}^{(1)} \\ -f_{010}^{(2)} & -\left(f_{100}^{(2)} + f_{001}^{(2)}\right) \end{bmatrix} \begin{bmatrix} U_2^{(1)} \\ U_2^{(2)} \end{bmatrix} = \begin{bmatrix} R_2 \\ R_6 \end{bmatrix}. \tag{52}$$

As a result, using Cramer's rule, it is obtained that

$$U_1^{(1)} = \frac{\det(j_{11})}{\det(j_1)},\ U_1^{(2)} = \frac{\det(j_{12})}{\det(j_1)},\ U_2^{(1)} = \frac{\det(j_{21})}{\det(j_2)},\ U_2^{(2)} = \frac{\det(j_{22})}{\det(j_2)}, \tag{53}$$

where

$$j_1 = \begin{bmatrix} 2i\theta - f_{10}^{(1)} & -f_{01}^{(1)} \\ -f_{010}^{(2)}\,e^{\,2i\theta\tau_0} & 2i\theta - (f_{100}^{(2)} + f_{001}^{(2)}\,e^{\,2i\theta\tau_0}) \end{bmatrix},$$

$$j_{11} = \begin{bmatrix} R_1 & -f_{01}^{(1)} \\ R_5 & 2i\theta - (f_{100}^{(2)} + f_{001}^{(2)}\,e^{\,2i\theta\tau_0}) \end{bmatrix},$$

$$j_{12} = \begin{bmatrix} -f_{10}^{(1)} & R_1 \\ -f_{010}^{(2)} & R_5 \end{bmatrix},\ j_2 = \begin{bmatrix} -f_{10}^{(1)} & -f_{01}^{(1)} \\ -f_{010}^{(2)} & -\left(f_{100}^{(2)} + f_{001}^{(2)}\right) \end{bmatrix},$$

$$j_{21} = \begin{bmatrix} R_2 & -f_{01}^{(1)} \\ R_6 & -\left(f_{100}^{(2)} + f_{001}^{(2)}\right) \end{bmatrix}, j_{22} = \begin{bmatrix} -f_{10}^{(1)} & R_2 \\ -f_{010}^{(2)} & R_6 \end{bmatrix},$$

Therefore, it becomes easy to find the value of both $W_{20}(x)$ and $W_{11}(x)$ in equation (50) using the obtained results from equation (53). Hence, the values of g_{21} in equation (49) can be determined. Finally, utilizing the determined value of g_{ij}, the value of the fixed quantities in equation (33) is obtained, then all the properties of the bifurcating Hopf bifurcation follow and the

proof is complete.

7. NUMERICAL SIMULATION

In this section, the main results is illustrated numerically using the following biologically feasible hypothetical set of parameters set. The objective is confined the theoretical obtained results and understand the influence of the parameters on the dynamics of the system (3).

$$r = 1, K = 10, a_1 = 0.5, \beta_1 = 2, a_2 = 0.32, b_1 = 0.1, \\ c = 0.15, b_2 = 0.4, \beta_2 = 2, m = 0.8, \tau = 0.1 \quad . \tag{54}$$

It is obtained that, the trajectory of the system (3) utilizing the parameters set (54) is approached to the coexistence equilibrium point $P_3 = (4.16,7.19)$ starting from different initial points, see Figure (1).

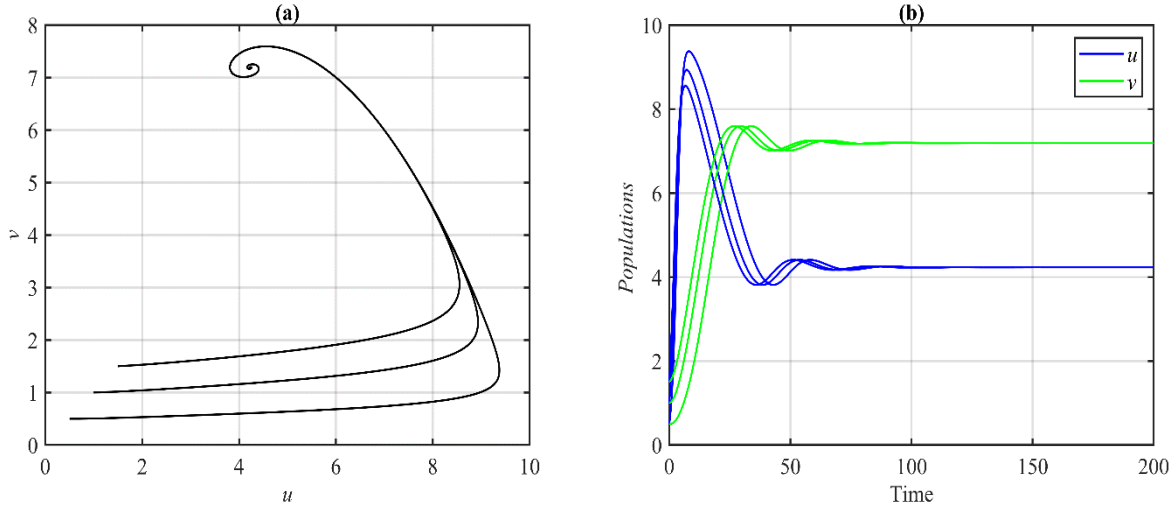

Figure 1: The trajectories of system (3) using the parameters set (54) with different initial points. (a) The phase portrait. (b) The time series.

The influence of the time delay is studied in Figure (2), the occurrence of Hopf bifurcation is clearly shown in that Figure at the bifurcation point $\tau_0 = 6.3$.

According to Figure (2), system (3) undergoes a Hopf bifurcation as the parameters τ pass through the value $\tau_0 = 6.3$. The periodic dynamics are asymptotic stable and become larger as the value of τ increases.

The influence of the varying other parameters is investigated in the following Figures. It is observed that, for the ranges $r \in (0,0.15]$, $r \in [0.16,0.81]$, and $r \geq 0.82$ the system (3) approaches asymptotically to P_3, limit cycle, and P_3 respectively as shown in the Figure (3) for the typical values of r.

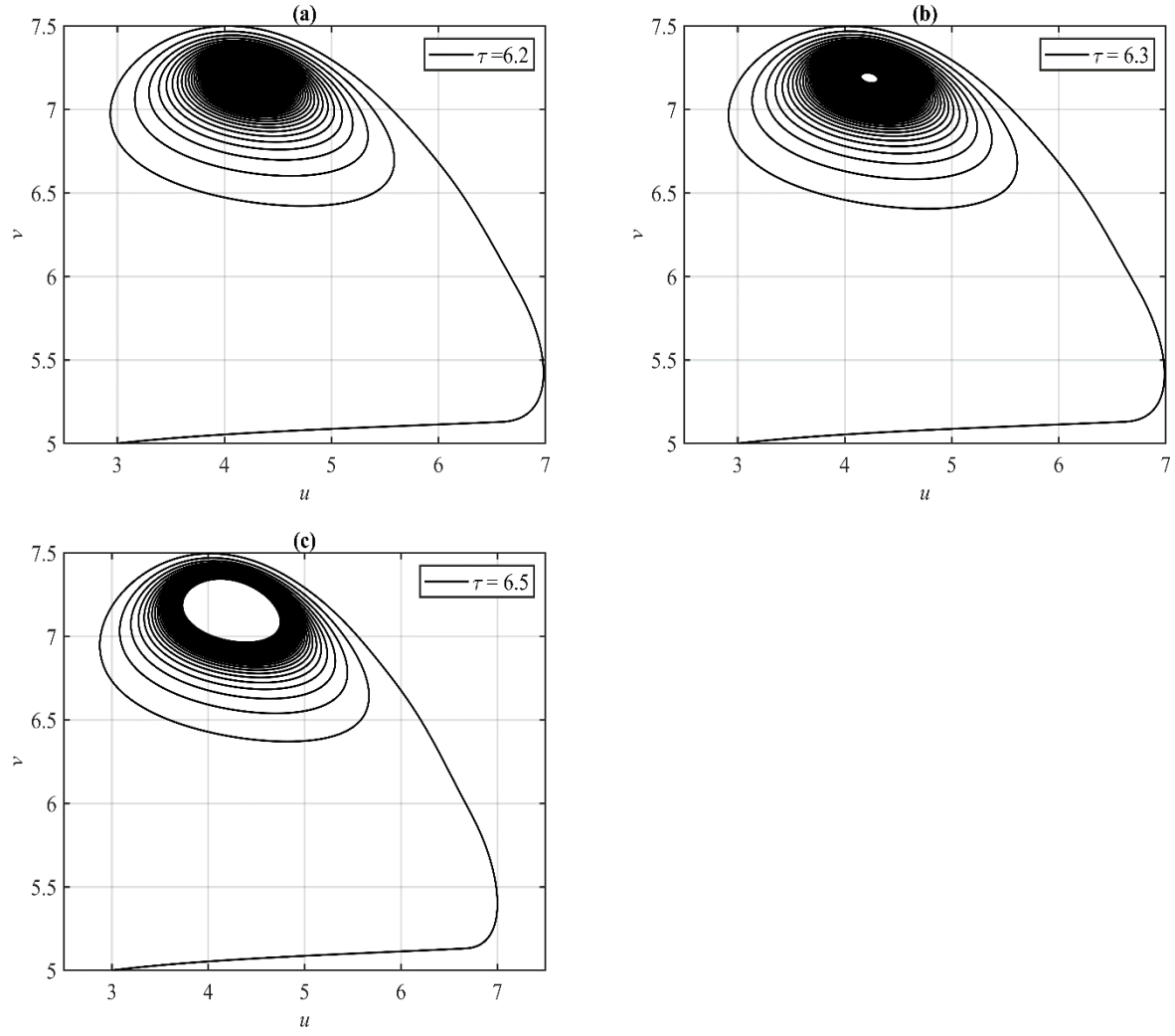

Figure 2: The trajectory of the system (3) using the parameters set (54) with different values of time delay shows the occurrence of Hopf bifurcation.

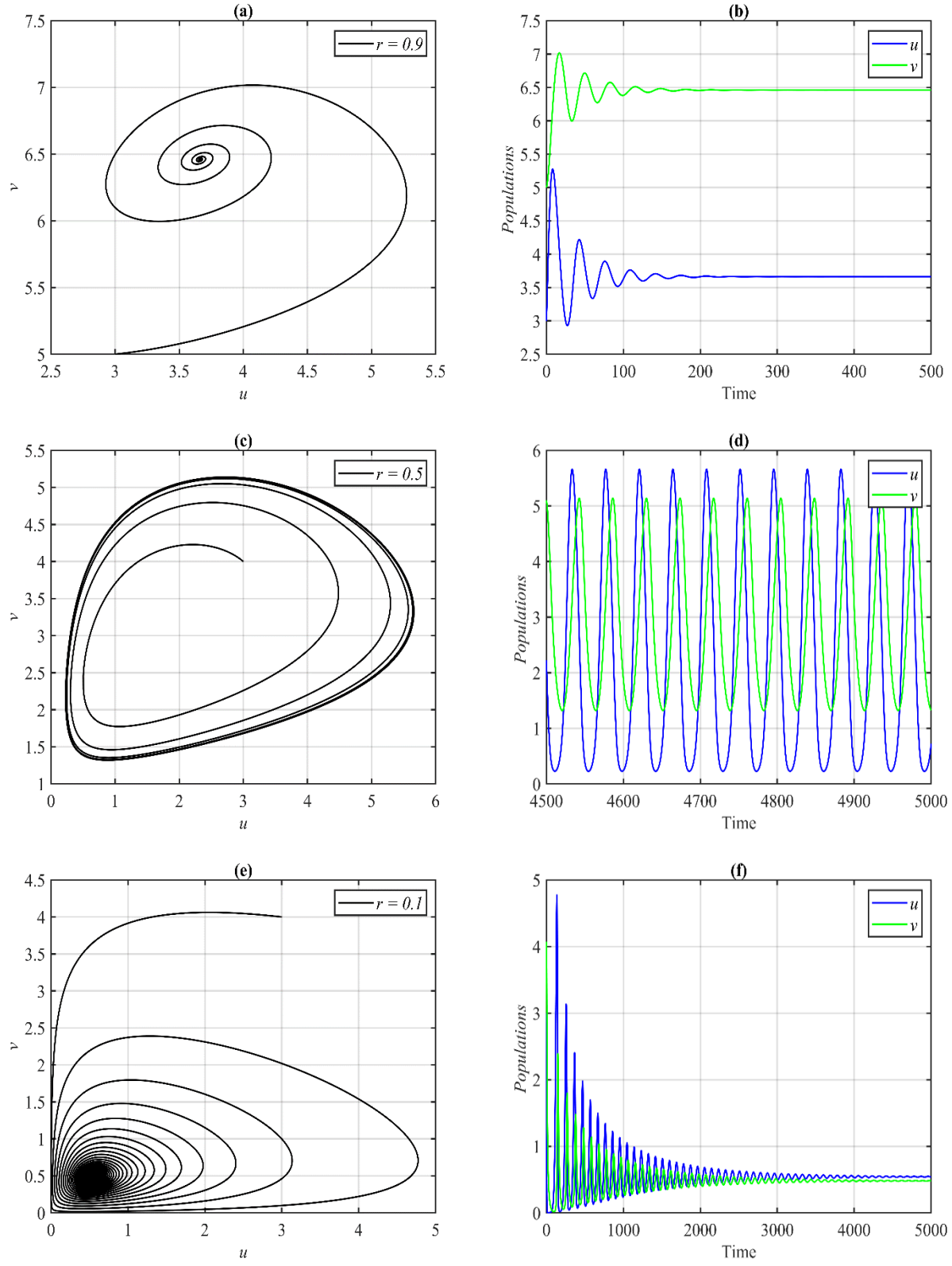

Figure 3: The trajectory of system (3) using the parameters set (54) with different values of r. (a) Asymptotic stable point $P_3 = (3.65,6.45)$ for $r = 0.9$. (b) Time series for $r = 0.9$. (c) Asymptotic stable limit cycle for $r = 0.5$. (d)

Time series for $r = 0.5$. (e) Asymptotic stable point $P_3 = (0.54,0.48)$ for $r = 0.1$. (b) Time series for $r = 0.1$.

For the parameter K, it is observed that for the ranges $K \in (0,0.37]$, and $K \geq 0.38$ system (3) approaches asymptotically to P_1, and P_3 respectively as shown in Figure (4) for the typical values of K.

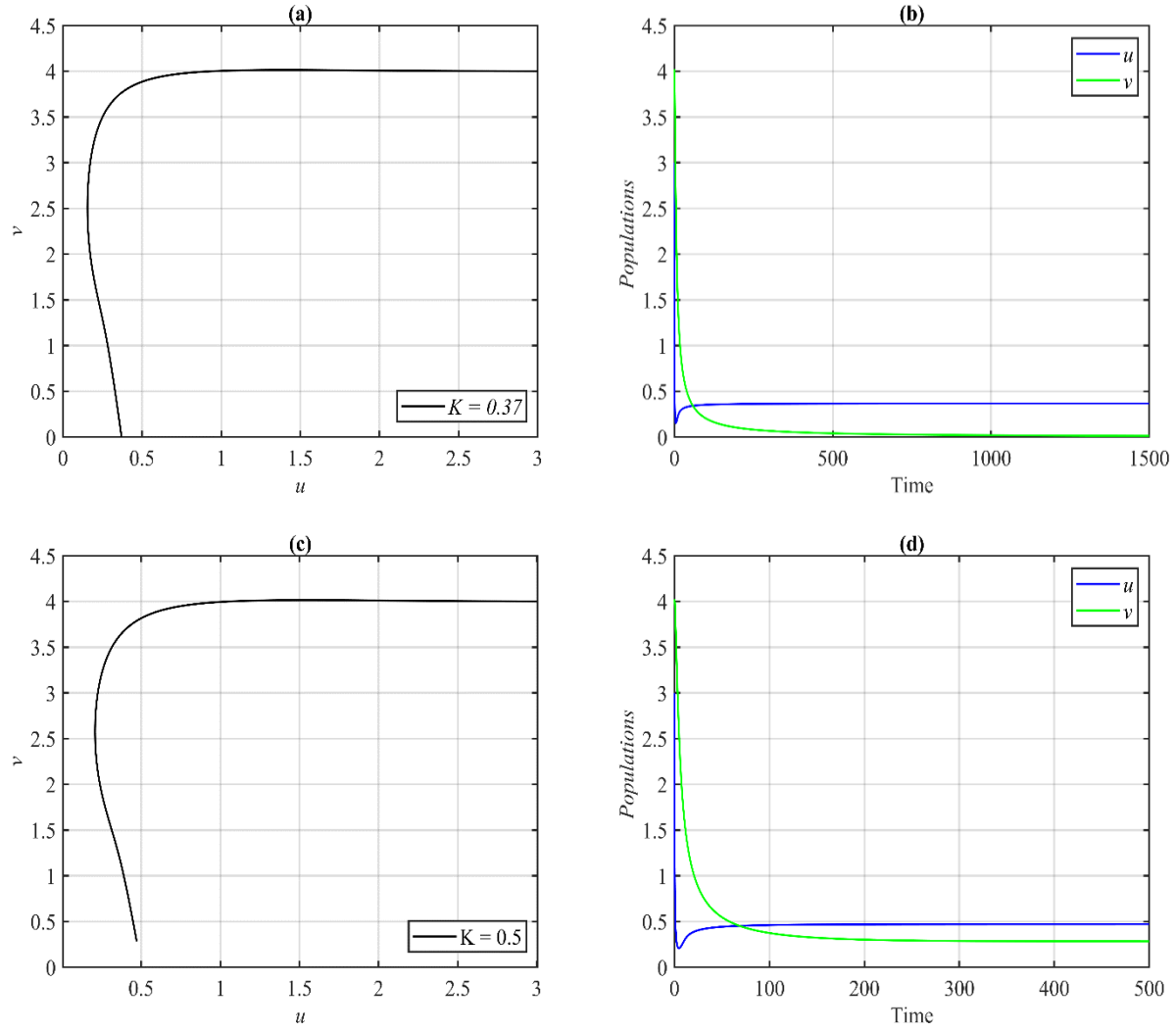

Figure 4: The trajectory of system (3) using the parameters set (54) with different values of K. (a) Asymptotic stable point $P_1 = (0.37,0)$ for $K = 0.37$. (b) Time series for $K = 0.37$. (c) Asymptotic stable $P_1 = (0.47,0.28)$ for $K = 0.5$. (d) Time series for $K = 0.5$.

Now for the parameter a_1, it is observed that, for the ranges $a_1 \in (0,0.59]$, and $a_1 \geq 0.6$ system (3) approaches asymptotically to P_3, and stable limit cycle respectively as shown in the Figure (5) for the typical values of a_1.

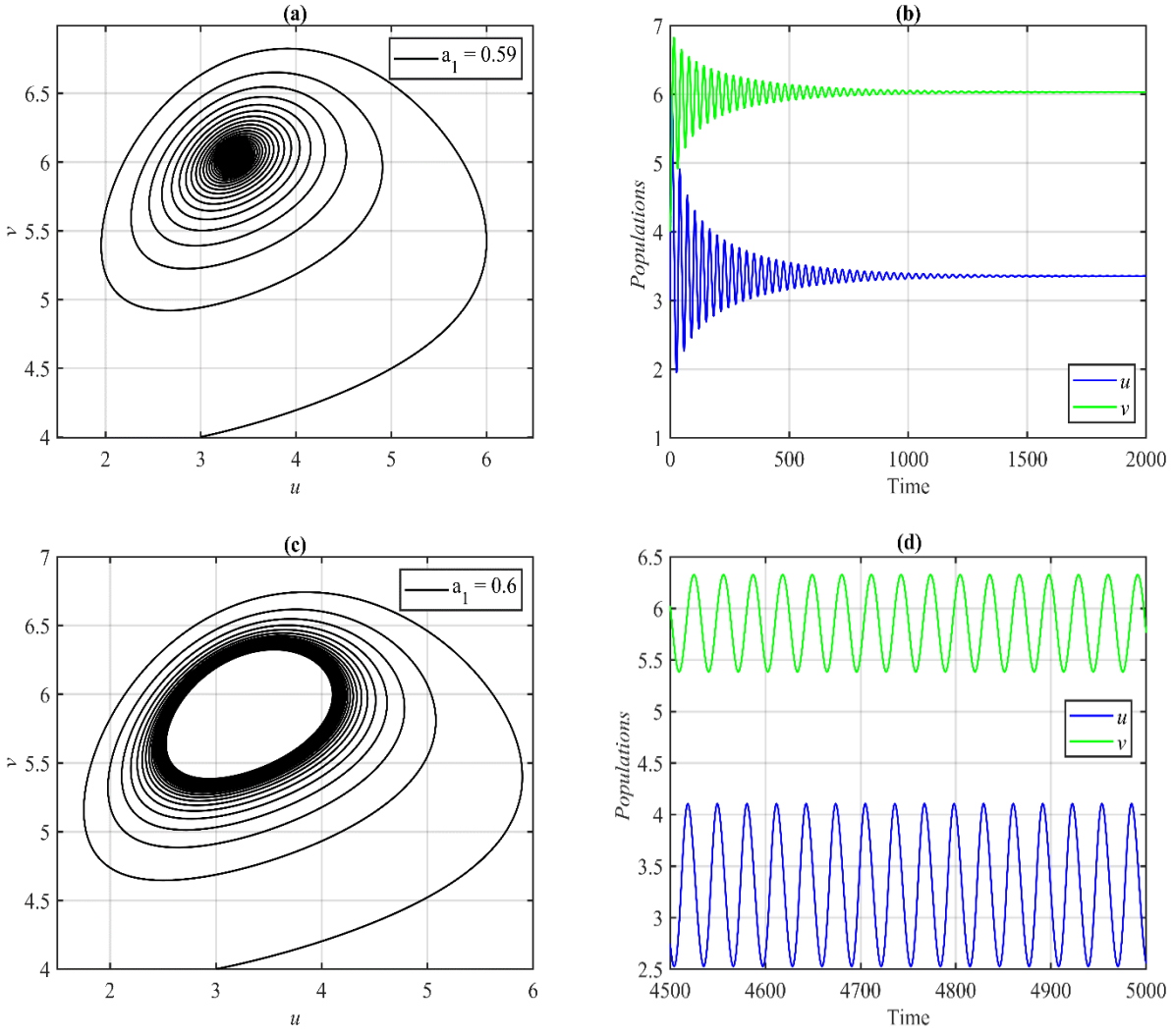

Figure 5: The trajectory of system (3) using the parameters set (54) with different values of a_1. (a) Asymptotic stable point $P_3 = (3.35,6.03)$ for $a_1 = 0.59$. (b) Time series for $a_1 = 0.59$. (c) Asymptotic stable limit cycle for $a_1 = 0.6$. (d) Time series for $a_1 = 0.6$.

For the parameter β_1, it is observed that, for the ranges $\beta_1 \in (0,1.75]$, and $\beta_1 \geq 1.76$ system (3) approaches asymptotically to a stable limit cycle, and P_3 respectively as shown in the Figure (6) for the typical values of β_1.

Moreover, for the parameter a_2, it is observed that, for the ranges $a_2 \in (0,0.06]$, $a_2 \in [0.07,0.34]$, and $0.35 \leq a_2 \leq a_1$ system (3) approaches asymptotically P_1, P_3, and a stable limit cycle respectively as shown in the Figure (7) for the typical values of a_2.

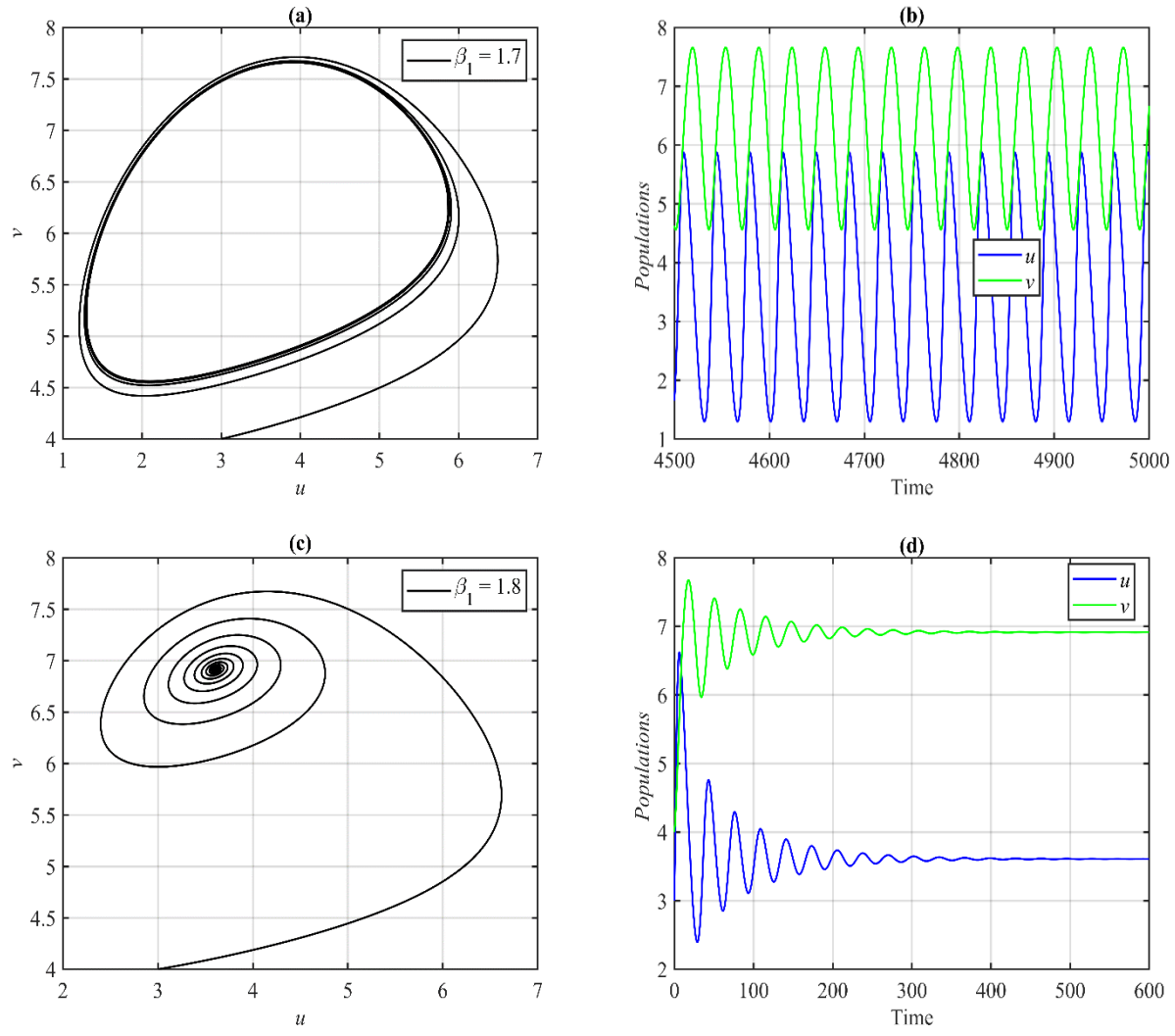

Figure 6: The trajectory of system (3) using the parameters set (54) with different values of β_1. (a) Asymptotic stable limit cycle for $\beta_1 = 1.7$. (b) Time series for $\beta_1 = 1.7$. (c) Asymptotic stable point $P_3 = (3.6,6.91)$ for $\beta_1 = 1.8$. (d) Time series for $\beta_1 = 1.8$.

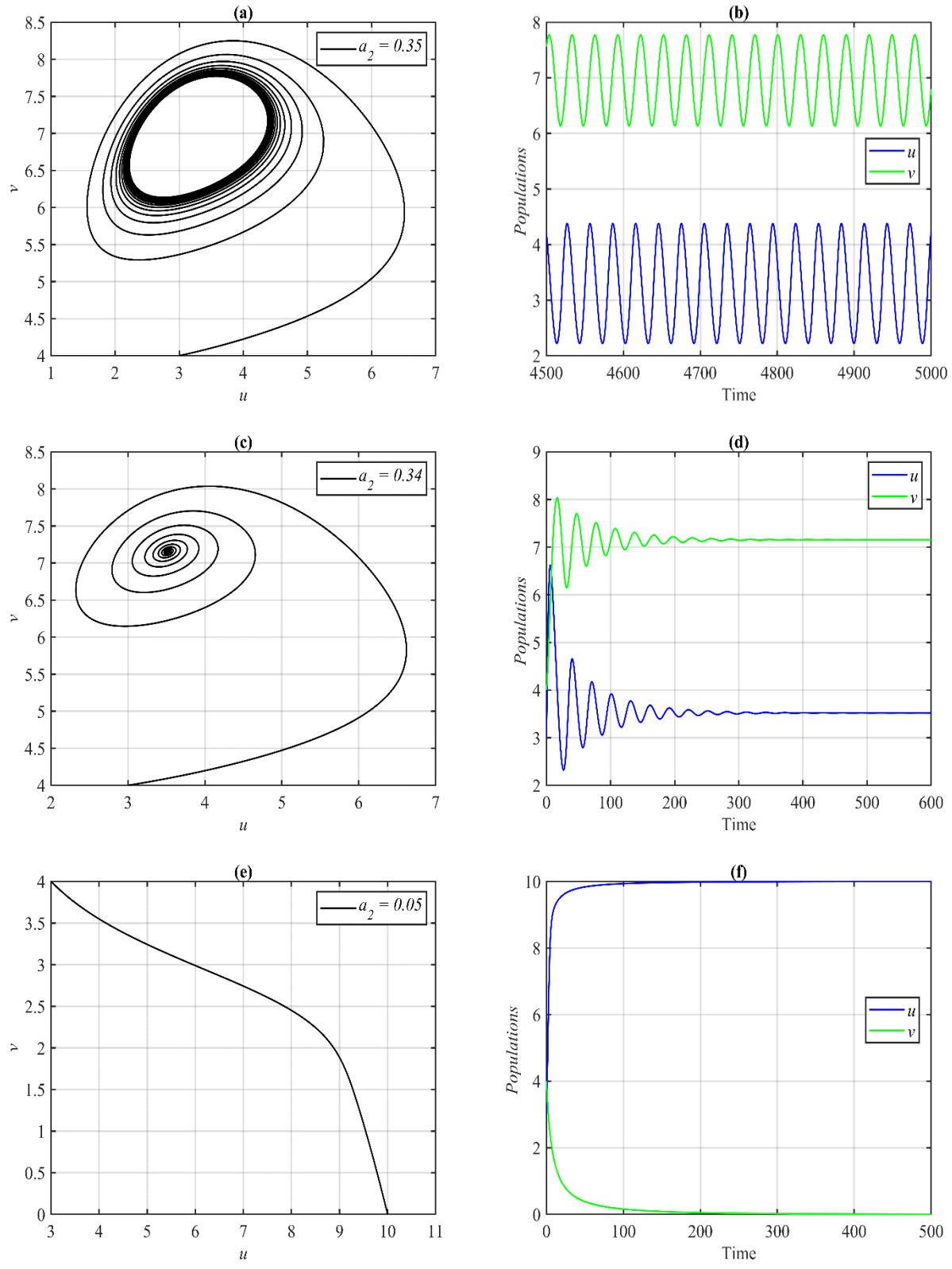

Figure 7: The trajectory of system (3) using the parameters set (54) with different values of a_2. (a) Asymptotic stable limit cycle for $a_2 = 0.35$. (b) Time series for $a_2 = 0.35$. (c) Asymptotic stable point $P_3 = (3.52,7.15)$ for $a_2 =$

0.34. (d) Time series for $a_2 = 0.34$. (e) Asymptotic stable point $P_1 = (10,0)$ for $a_2 = 0.05$. (f) Time series for $a_2 = 0.05$.

For the parameter b_1, it is observed that, for the ranges $b_1 \in (0,0.11]$, $b_1 \in [0.12,0.23]$, $b_1 \in [0.24,0.26]$, and $0.27 \leq b_1$ system (3) approaches asymptotically P_3, a stable limit cycle, P_3, and P_2 respectively as shown in the Figure (8) for the typical values of b_1.

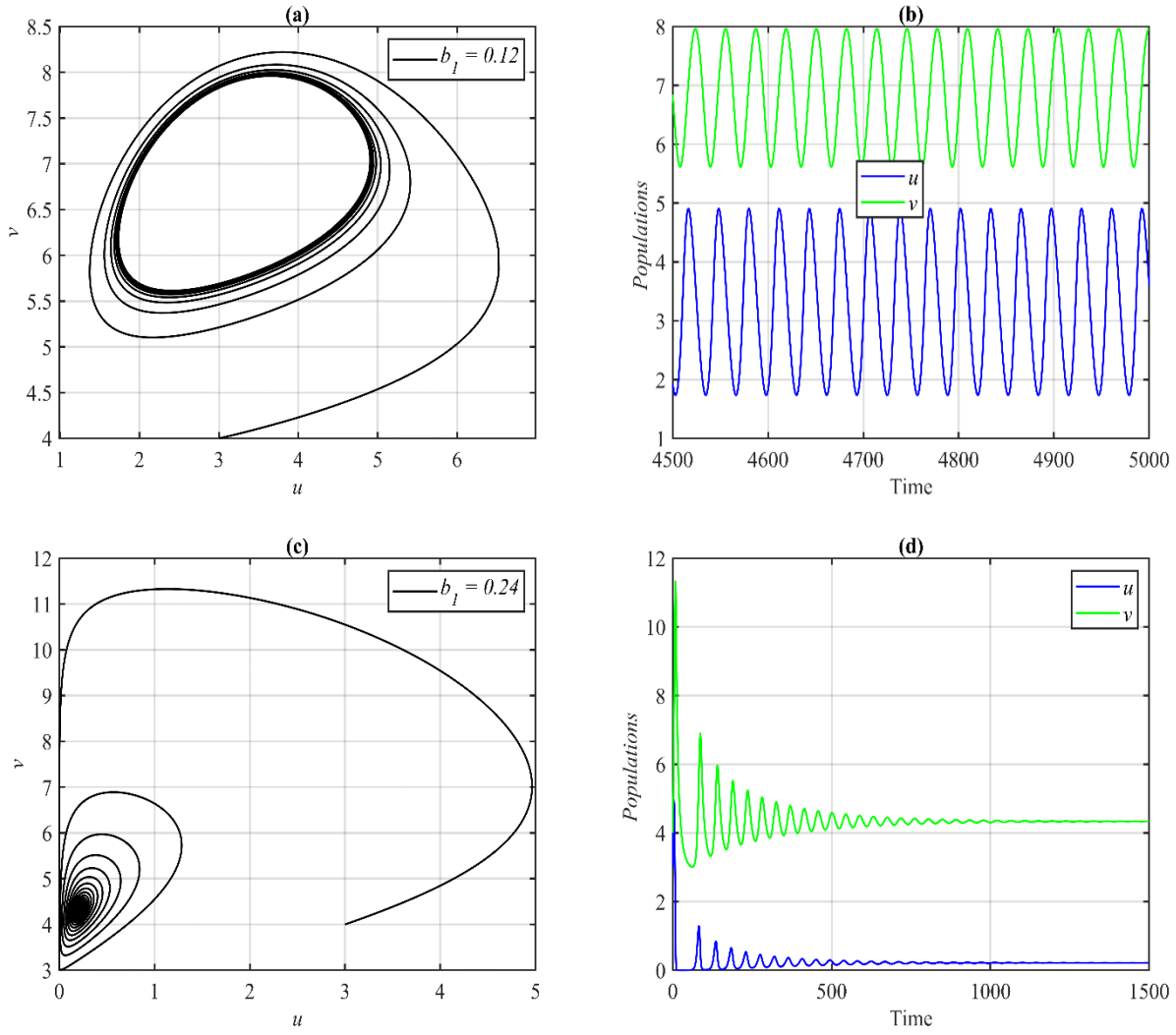

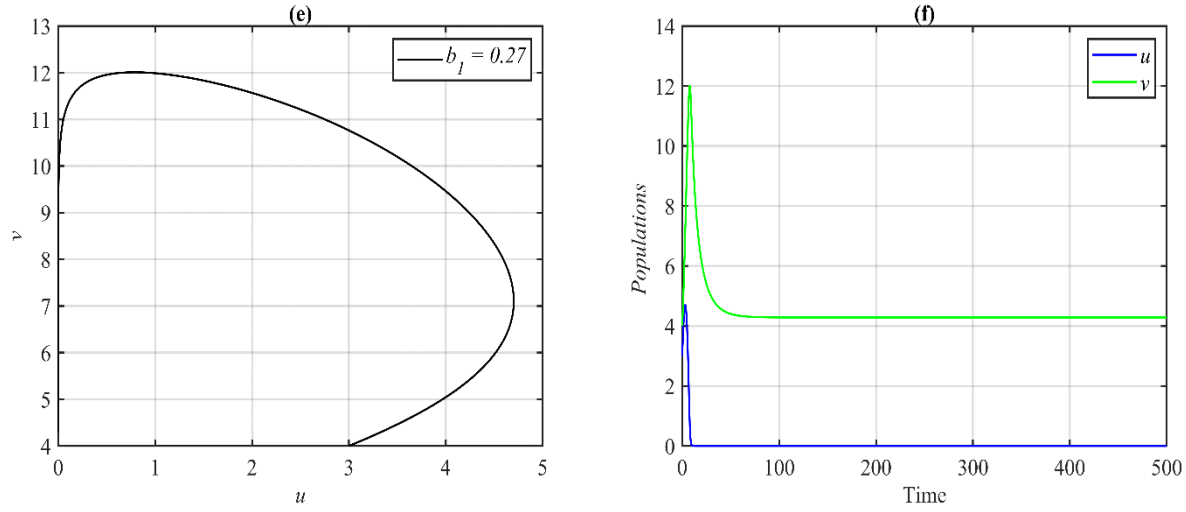

Figure 8: The trajectory of system (3) using the parameters set (54) with different values of b_1. (a) Asymptotic stable limit cycle for $b_1 = 0.12$. (b) Time series for $b_1 = 0.12$. (c) Asymptotic stable point $P_3 = (0.21,4.33)$ for $b_1 = 0.24$. (d) Time series for $b_1 = 0.24$. (e) Asymptotic stable point $P_2 = (0,4.28)$ for $b_1 = 0.27$. (f) Time series for $b_1 = 0.27$.

Now, for the parameter c, it is observed that, for the ranges $c \in (0,0.012]$, $c \in [0.013,0.13]$, $c \in [0.14,0.36]$, and $0.37 \leq c$ system (3) approaches asymptotically P_3, a stable limit cycle, P_3, and P_1 respectively as shown in the Figure (9) for the typical values of c.

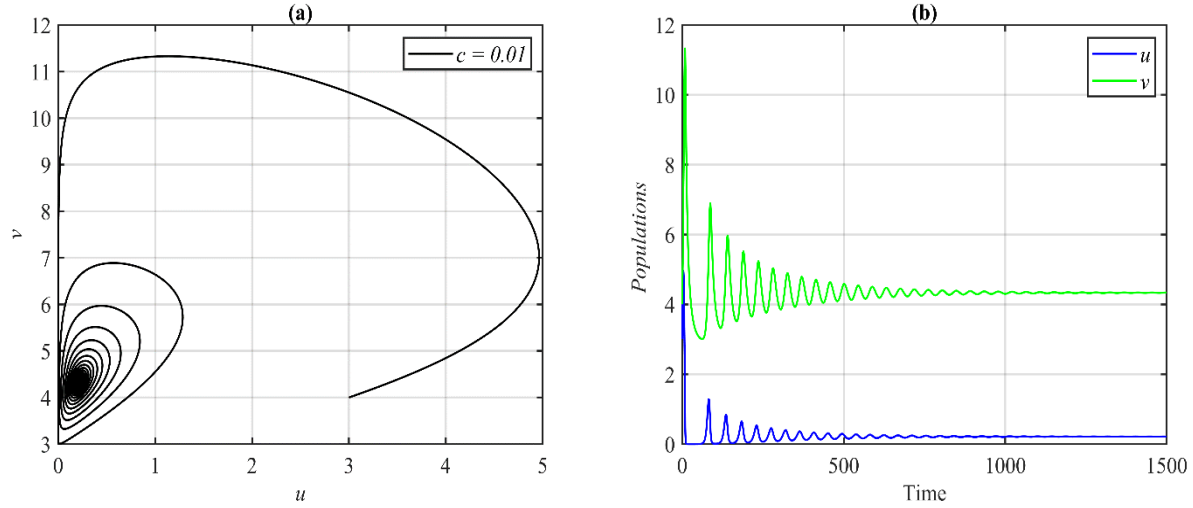

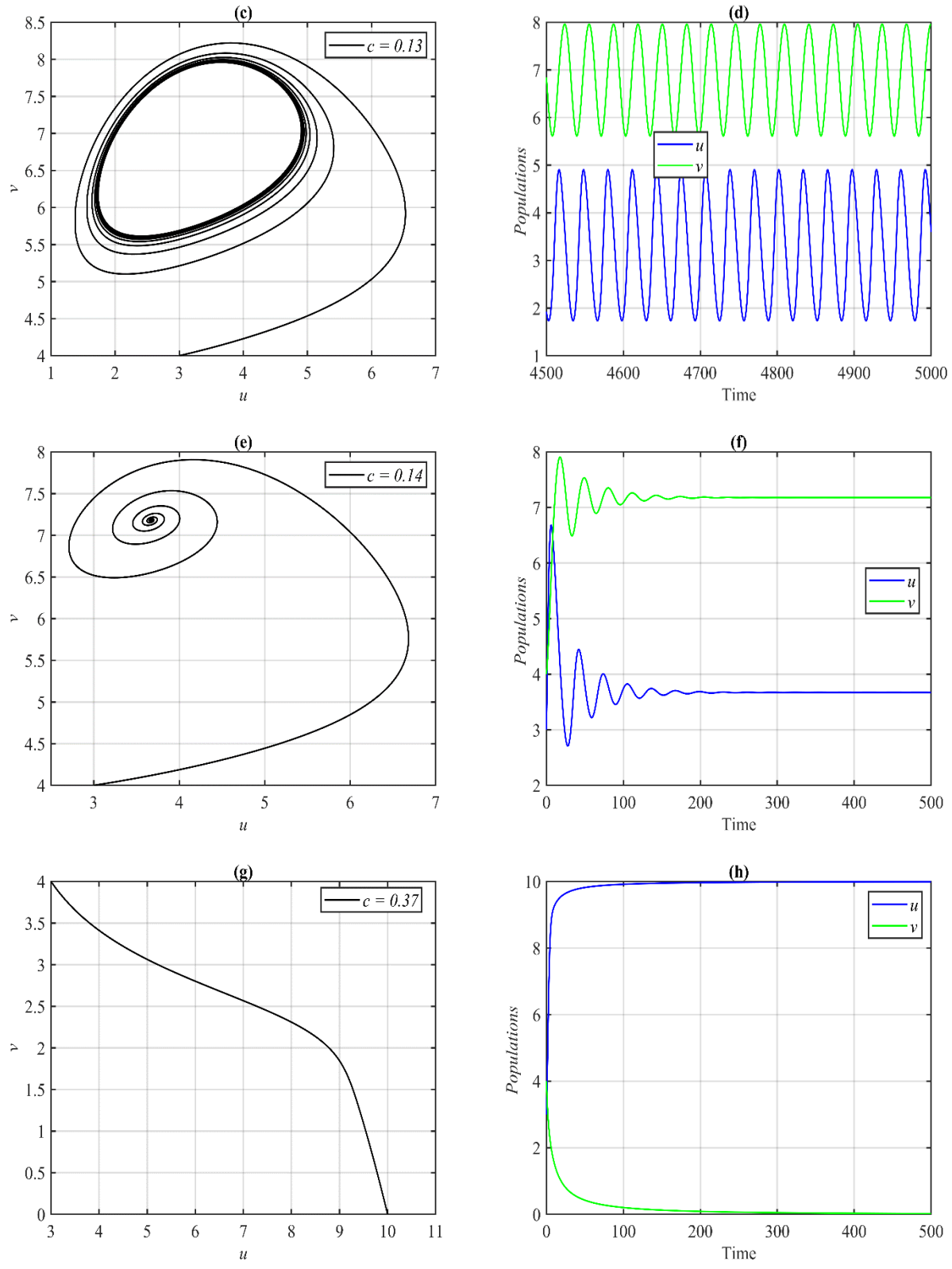

Figure 9: The trajectory of system (3) using the parameters set (54) with different values of c. (a) Asymptotic stable point $P_3 = (0.21,4.33)$ for $c = 0.01$. (b) Time series for $c = 0.01$. (c) Asymptotic stable limit cycle for $c = 0.13$.

(d) Time series for $c = 0.13$. (e) Asymptotic stable point $P_3 = (3.64,7.2)$ for $c = 0.14$. (f) Time series for $c = 0.14$. (g) Asymptotic stable point $P_1 = (10,0)$ for $c = 0.37$. (h) Time series for $c = 0.37$.

Finally, it is observed that the influence of other parameters on the system's dynamics (3) is similar to some of the above parameters, and Table (1) summarizes them.

Table 1: The dynamics of the system (3) as a function of the parameter

The parameter	Its range	The dynamics
b_2	$b_2 \in (0,0.36]$	The system (3) approaches asymptotically to limit cycle
	$b_2 \geq 0.37$	The system (3) approaches asymptotically to P_3
β_2	$\beta_2 \in (0,0.0005]$	The system (3) approaches asymptotically to P_1
	$\beta_2 \in [0.0006,0.38]$	The system (3) approaches asymptotically to P_3
	$\beta_2 \geq 0.39$	The system (3) approaches asymptotically to limit cycle
m	$m \in (0,0.83]$	The system (3) approaches asymptotically to P_3
	$m \in [0.84,1)$	The system (3) approaches asymptotically to limit cycle

8. CONCLUSIONS

In this paper, a model describing a delayed prey-predator interaction that incorporates predator cannibalism and refuge is investigated. The Holling type II functional response was used to describe the predation and cannibalism processes. All the system solution properties are discussed. It is obtained that, system (3) has four possible nonnegative equilibrium points. The local stability of them are studied for $\tau \geq 0$, and the stability conditions are determined. The existence of Hopf bifurcation as a function of τ is proved. The stability and direction of the bifurcated periodic dynamics is investigated using the center manifold and normal form theory. Finally, numerical simulation was used to verified the obtained results and understand the influence of varying system's parameters using hypothetical set of parameters values. The following conclusions are obtained numerically depending on the parameters set (54).

1. The system has two types of attractors, stable point or else stable limit cycle depending on the set of parameters used. For set (54), the system approaches asymptotically to the coexistence equilibrium point from different initial points.
2. The system undergoes a Hopf bifurcation as the parameter τ passing the bifurcation point $\tau_0 = 6.3$.

3. The system approaches the coexistence equilibrium point with large values of intrinsic growth rates asymptotically. While decreasing this parameter destabilizes the coexistence point and periodic dynamics obtained. It is observed that lowering the intrinsic growth rate further returns the system stability at the coexistence point.
4. Increasing the carrying capacity keeps the system stability at the coexistence point, while, decreasing it below a specific value causing extinction in a predator and the system approaches to predator-free point.
5. Increasing the predation rate above a specific value destabilizes the coexistence equilibrium point and the system approaches periodic dynamics. A similar effect had been shown with increasing the predator refuge constant.
6. Decreasing the predation half-saturation constant below a specific value destabilizes the coexistence equilibrium point and the system approaches periodic dynamics. A similar effect had been shown with decreasing the cannibalism rate.
7. Increasing the conversion rate above a specific value causes destabilizing the coexistence equilibrium point and the system approaches a stable limit cycle. However, decreasing it below a threshold value leads to extinction in predator species and the system comes asymptotically to a predator-free point. A similar effect had been shown with varying the cannibalism half-saturation constant.
8. With the exception of the existence of a threshold value at which the system approaches an asymptotically prey-free equilibrium point, the cannibalism conversion rate has effects on the system dynamics that are comparable to those observed with an intrinsic growth rate.
9. With the exception of the existence of a threshold value at which the system approaches an asymptotically predator-free equilibrium point, the predator death rate has comparable effects on the system's dynamics as those demonstrated with an intrinsic growth rate.

CONFLICT OF INTERESTS

The author(s) declare that there is no conflict of interests.

REFERENCES

[1] L.R. Fox, Cannibalism in natural populations, Annu. Rev. Ecol. Syst. 6 (1975), 87-106. https://doi.org/10.1146/annurev.es.06.110175.000511.

[2] S. Biswas, S. Chatterjee, J. Chattopadhyay, Cannibalism may control disease in predator population: result drawn

from a model based study, Math. Meth. Appl. Sci. 38 (2014), 2272-2290. https://doi.org/10.1002/mma.3220.

[3] Y. Jia, Y. Li, J. Wu, Effect of predator cannibalism and prey growth on the dynamic behavior for a predator-stage structured population model with diffusion, J. Math. Anal. Appl. 449 (2017), 1479-1501. https://doi.org/10.1016/j.jmaa.2016.12.036.

[4] H. Deng, F. Chen, Z. Zhu, Z. Li, Dynamic behaviors of Lotka–Volterra predator–prey model incorporating predator cannibalism, Adv. Differ. Equ. 2019 (2019), 359. https://doi.org/10.1186/s13662-019-2289-8.

[5] F. Zhang, Y. Chen, J. Li, Dynamical analysis of a stage-structured predator-prey model with cannibalism, Math. Biosci. 307 (2019), 33-41. https://doi.org/10.1016/j.mbs.2018.11.004.

[6] M. Nishikawa, N. Ferrero, S. Cheves, et al. Infant cannibalism in wild white-faced capuchin monkeys, Ecol. Evol. 10 (2020), 12679-12684. https://doi.org/10.1002/ece3.6901.

[7] M. Rayungsari, A. Suryanto, W.M. Kusumawinahyu, et al. Dynamical analysis of a predator-prey model incorporating predator cannibalism and refuge, Axioms. 11 (2022) 116. https://doi.org/10.3390/axioms11030116.

[8] S. Kundu, S. Maitra, Dynamical behaviour of a delayed three species predator–prey model with cooperation among the prey species, Nonlinear Dyn. 92 (2018), 627-643. https://doi.org/10.1007/s11071-018-4079-3.

[9] X. Zhang, Z. Liu, Hopf bifurcation analysis in a predator-prey model with predator-age structure and predator-prey reaction time delay, Appl. Math. Model. 91 (2021), 530-548. https://doi.org/10.1016/j.apm.2020.08.054.

[10] K. Sarkar, S. Khajanchi, P.C. Mali, A delayed eco-epidemiological model with weak Allee effect and disease in prey, Int. J. Bifurcation Chaos. 32 (2022), 2250122. https://doi.org/10.1142/s021812742250122x.

[11] R.M. Hussien, R.K. Naji, The dynamics of a delayed ecoepidemiological model with nonlinear incidence rate, J. Appl. Math. 2023 (2023), 1366763. https://doi.org/10.1155/2023/1366763.

[12] C.S. Holling, The functional response of predators to prey density and its role in mimicry and population regulation, Mem. Entomol. Soc. Can. 97 (1965), 5–60. https://doi.org/10.4039/entm9745fv.

[13] N. Bairagi, P.K. Roy, J. Chattopadhyay, Role of infection on the stability of a predator–prey system with several response functions—A comparative study, J. Theor. Biol. 248 (2007), 10-25. https://doi.org/10.1016/j.jtbi.2007.05.005.

[14] D. Mukherjee, C. Maji, Bifurcation analysis of a Holling type II predator-prey model with refuge, Chinese J. Phys. 65 (2020), 153-162. https://doi.org/10.1016/j.cjph.2020.02.012.

[15] H. Molla, Md. Sabiar Rahman, S. Sarwardi, Dynamics of a predator-prey model with Holling type II functional response incorporating a prey refuge depending on both the species, Int. J. Nonlinear Sci. Numer. Simul. 20 (2018), 89-104. https://doi.org/10.1515/ijnsns-2017-0224.

[16] J. Ye, J. Li, Factors affecting cannibalism by Mallada basalis, Biocontrol Sci. Technol. 30 (2020), 442-450. https://doi.org/10.1080/09583157.2020.1729700.

[17] A.S. Abdulghafour, R.K. Naji, Modeling and analysis of a prey-predator system incorporating fear, predator-dependent refuge, and cannibalism, Commun. Math. Biol. Neurosci. 2022 (2022), 106. https://doi.org/10.28919/cmbn/7722.

[18] H. Freedman, V. Rao, The trade-off between mutual interference and time lags in predator-prey systems, Bull. Math. Biol. 45 (1983), 991-1004. https://doi.org/10.1016/s0092-8240(83)80073-1.

[19] S. Ruan, On the zeros of a third degree exponential polynomial with applications to a delayed model for the control of testosterone secretion, Math. Med. Biol. 18 (2001), 41-52. https://doi.org/10.1093/imammb/18.1.41.

[20] B.D. Hassard, N.D. Kazarinoff, Y.H. Wan, Theory and applications of Hopf bifurcation, Cambridge University Press, Cambridge, 1981.